

# Ionospheric Modeling at North-East Asia using IGS sites

\*Byung-Kyu Choi<sup>1</sup>, Jong-Uk Park<sup>2</sup> and Sang-Jeong Lee<sup>3</sup>

<sup>1</sup>GNSS Technology Group, Korea Astronomy and Space Science Insititute(E-mail: bkchoi@kasi.re.kr )

<sup>2</sup>GNSS Technology Group, Korea Astronomy and Space Science Insititute(E-mail: jupark@kasi.re.kr )

<sup>3</sup> Electronics Engineering, Chungnam Nat'l Univ.(E-mail: essjl@cnu.ac.kr)

## Abstract

One of the major sources of error in precise GPS positioning since the turn-off the Selective Availability(SA) is the ionospheric propagation delay. For the last decades, a lot of the ionospheric researches based on a GPS network have been implemented throughout the world. Especially researches of the ionospheric modeling for Wide Area Argumentation System(WAAS) have been undertaken and published. In mid-latitude regions, typical spatial and temporal variations in ionospheric models delay tend to minimal. The developed ionospheric model calls for a 1.25 degree grid at latitudes and a 2.5 degree grid at longitudes. The precise grid TEC estimated by the inversion technique is also compared with global ionosphere maps(GIMs) which have been provided by several analysis centers(ACs). The results of initial investigations into the suitability of the proposed ionospheric modeling scheme in north-east Asia are presented.

**Keywords:** Ionospheric modeling, WAAS, TEC, GIMs

## 1. Introduction

In the last decade, GPS has become a valuable tool for determining total electron contents(TEC) of ionosphere. In order to study the characteristics of ionosphere, The global and regional GPS networks have been commonly used. Dual-frequency observations of GPS signals provide a relative ionospheric delay of the two-frequency electromagnetic waves traveling through a dispersive medium. The TEC along the line of sight can be derived from this delay(Lanyi et al.(1998)). The currently available ionosphere correction models include the Klobuchar ionosphere parameters from the GPS satellites, but the Klobuchar model could only correct about 50% of the total ionosphere effects(Klobuchar, 1987). Therefore more precise ionosphere model is necessary. Ionospheric model using GPS networks has been widely developed over the past 10 years(Komjathy, 1997; Skone, 1998; Jakowski et al., 1998; Liao, 2000; Fedrizzi et al., 2001).

All proposed ionospheric models could be classified into two different categories : grid-based and functional-based. The functional-based models are based on the function fitting techniques such as the broadcast ionosphere model from the GPS satellites(Klobuchar, 1987), the spherical harmonics(Schaer, 1999; Walker, 1989) and the polynomial functions(Coster et al., 1992; Komjathy, 1997). Recently, the increase of IGS sites and that of the regional GPS networks plays on key rule on studying ionospheric irregularities. The global and regional GPS networks have contributed to the research like this with different time and spatial resolution(Wilson et al., 1995; Leonovich et al., 2000)

In general, The global ionospheric model using the worldwide GPS network is modeled by the expansion of spherical harmonic functions, also called Global Ionosphere Maps(GIMs). Most of this models have been developed by International Associate Analysis Centers(IAACs) which were involved CODE/Univ. Bern, ESA, JPL, NRCAN and UPC and released to public users with IONEX format(each 2 hours, 5 by 2.5 deg. in longitude and latitude).

## 2. Background

### 2.1 TEC Calculation

Basically, in order to estimate the electron density distribution with height of ionosphere, the calculation for slant TEC (STEC) or vertical TEC (VTEC) has to be initially implemented (Hernandez et al. (1999)). When using the dual-frequency GPS data, it is available to estimate precisely the TEC. Code measurements (P1,P2) are expressed as follows (Gao et al. (2002)).

$$P1(k) = \rho + c(\delta t^s - \delta t_r) + \frac{40.3}{f_1^2} TEC(k) + \varepsilon_{trop} + \varepsilon_m + \varepsilon_{L1} \quad (1)$$

$$P2(k) = \rho + c(\delta t^s - \delta t_r) + \frac{40.3}{f_2^2} TEC(k) + \varepsilon_{trop} + \varepsilon_m + \varepsilon_{L2} \quad (2)$$

where  $\rho$  is the true geometric range between receiver and satellite (m),  $\delta t^s$  is the satellite clock error with respect to GPS time (s),  $\delta t_r$  is the receiver clock error with respect to GPS time (s).  $\varepsilon_{L_i}$  (i = 1, 2) is the noise on L1 and L2. On the occasion of using carrier phase data, the following linear combination equation is formed.

$$I_\phi(k) = \frac{f_1^2}{f_1^2 - f_2^2} \phi_1(k) - \frac{f_2^2}{f_1^2 - f_2^2} \phi_2(k) \quad (3)$$

where  $f_1$  (1575.42 MHz) and  $f_2$  (1227.60 MHz) are frequencies on L1 and L2 respectively.  $\phi_1$  and  $\phi_2$  are carrier phase measurements.

## 2.2 Ionosphere Pierce Point(IPP) Calculation

The IPP is the point where a ray from the receiver to a GPS satellite “punctures” the ionosphere at the altitude of maximum electron density (about 350~500km).

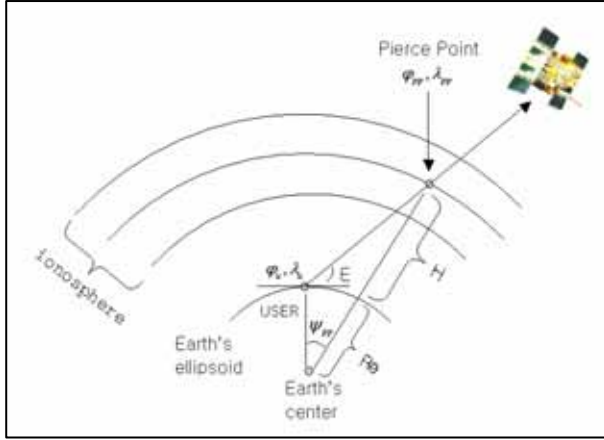


Figure 1. Ionosphere Pierce Point Diagram

In Figure 1,  $(\phi_u, \lambda_u)$  are the user's earth coordinates in latitude and longitude,  $E$  is the elevation to the satellite,  $R_e$  is the radius of the earth (taken to be 6378.136km),  $\psi_{pp}$  is the angle from the user to the IPP as measured from the center of the earth, and  $(\phi_{pp}, \lambda_{pp})$  are the earth coordinates of the IPP. The mathematical expression of IPP is described as follows

$$\psi_{pp} = \frac{\pi}{2} - E - \sin^{-1}\left(\frac{R_e}{R_e + h_i} \cos E\right) \quad (4)$$

$$\phi_{pp} = \sin^{-1}(\sin \phi_u \cos \psi_{pp} + \cos \phi_u \sin \psi_{pp} \cos A) \quad (5)$$

$$\lambda_{pp} = \lambda_u + \sin^{-1}\left(\frac{\sin \psi_{pp} \sin A}{\cos \phi_{pp}}\right) \quad (6)$$

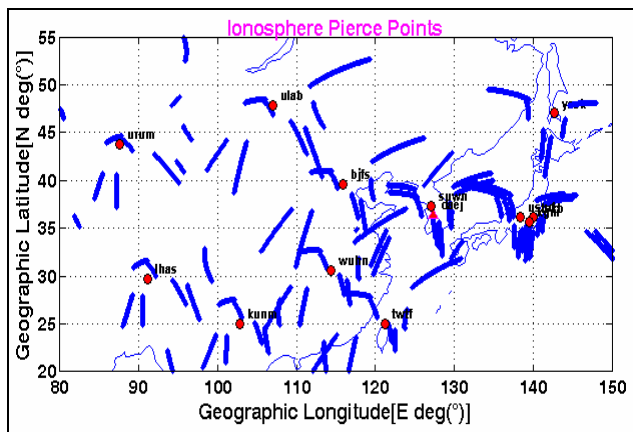


Figure 2. Monitoring of IPPs using IGS sites in Asia

Figure 2 shows the monitoring of IPPs for one temporal hour. It covers a region which locates between 80°-150°E in the geographic longitude and 20°-55°N in the geographic latitude. This designed area is covered by all IPPs for most of the

processed epochs, thus instantaneous ionosphere mapping is ensured. Red dots shown in Figure 2 represent the IGS stations used for north-east Asia ionosphere modeling. The coordinates of that are shown in Table 1.

Table 1. The precise coordinates of IGS site for north-east Asia ionospheric modeling

Name	X	Y	Z
BJFS	-2148743.7842	4426641.2359	4044655.9355
DAEJ	-3120041.7775	4084614.9702	3764027.0059
SUWN	-3062022.6527	4055448.0890	3841818.3399
TSKB	-3957199.2404	3310199.6682	3737711.7075
URUM	193030.8728	4606851.3241	4393311.4212
USUD	-3855262.9979	3427432.5194	3741020.3624
WUHN	-2267749.1617	5009154.3251	3221290.7616
YSSK	-3465320.7980	2638269.3995	4644085.4927
ULAB	-1257094.1341	4098399.8023	4706820.2769
LHAS	-106937.6693	5549269.5907	3139215.7619
TWTF	-2994427.9721	4951309.2924	2674496.9358
KGNI	-3941949.1592	3368156.3546	3702214.8303
KUNM	-1281255.4729	5640746.0787	2682880.1170
PIMO	-3186294.1703	5286624.0926	1601158.1764

IGS sites used to the data processing are : BJFS(39°N, 115°E), DAEJ(36°N, 127°E), SUWN(37°N, 127°E), TSKB(36°N, 140°E), URUM(43°N, 87°E), USUD(36°N, 138°E), WUHN(30°N, 114°E), YSSK(47°N, 142°E), ULAB(47°N, 107°E), LHAS(29°N, 91°E), TWTF(24°N, 121°E), KGNI(35°N, 139°E), KUNM(25°N, 102°E) and PIMO(14°N, 121°E). Total 14 IGS stations were considered.

## 2.3 Inverse Distance Weighted(IDW) application

One of the most commonly used techniques for interpolation of distributed points is inverse distance weighted(IDW) interpolation. Inverse distance weighted methods are based on the assumption that the interpolating surface should be influenced most by the nearby points and less by the more distance points. A simple IDW weighting factor is

$$w(d) = \frac{1}{d^p} \quad (7)$$

Where  $w(d)$  is the weighting factor applied to a known value,  $d$  is the distance from the known value to the unknown value, and  $p$  is a user-selected power factor. Here weight decreases as distance increase from the interpolated point. A general form of interpolating a value using IDW is as follows

$$z_0 = \frac{\sum_{i=1}^s z_i \cdot \frac{1}{d_i^k}}{\sum_{i=1}^s \frac{1}{d_i^k}} \quad (8)$$

Where  $z$  is the value of the interpolated point,  $z_i$  is a known value, and  $s$  is the total number of known points used in interpolation.

### 3. Data Processing Strategy

As mentioned above, ionosphere models have been developed by several methods and a variety of data. In order to estimate TEC in this research, IDW interpolation method was applied to data processing. Data processing scheme for ionospheric modeling is seen in Figure 3.

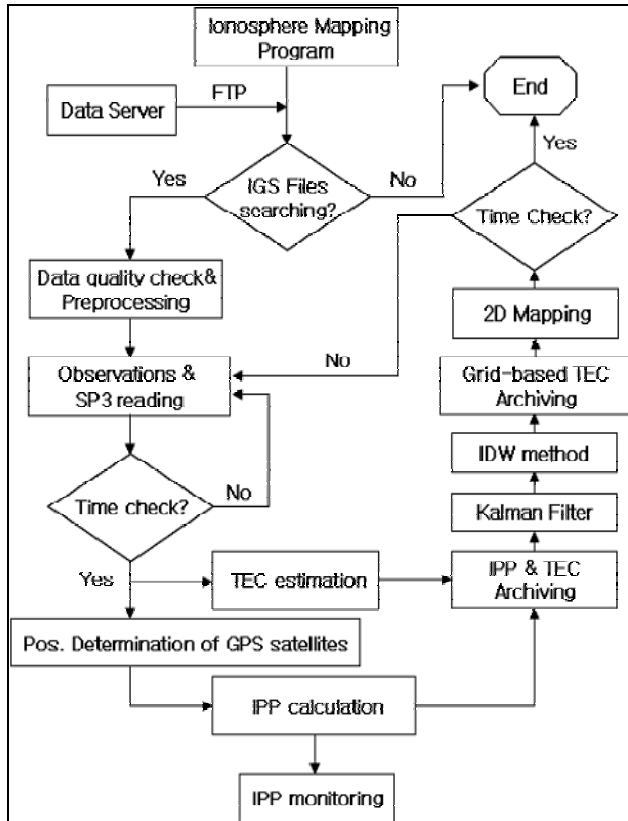


Figure 3. Data Processing Scheme

As seen in Figure 3, when the ionosphere mapping program is executed, the searching, quality checking and pre-processing of IGS data are implemented earlier than other works. To calculate the more precise TEC value, dual frequency measurement data are used simultaneously in a process of TEC estimation module. The positioning determination of GPS satellites uses Lagrange method expanded up to 10 degree.

One of the important things is to make efficient use of ionosphere pierce points. The estimated TEC values can be different by IPP calculation. Another purpose of IPPs monitoring is to evaluate the precise position of GPS satellites which can affect the variation of TEC. Next step is to archive TEC and IPP and then TEC values are complemented by Kalman Filter method and IDW interpolation. The developed program is also based on grid form which has a temporal resolution of 1.25° 2.5° in latitude and longitude regionally and 30 second time resolution.

### 4. Results

TEC in north-east Asia ionospheric model was estimated using IGS data for a temporal day. Each of grid point TEC was obtained and archived with the previously arranged spatial resolution. This modeling was conducted using IGS data observed from 14 IGS sites within north-east Asia on October 29, 2003. During this day, it was reported that the eruption of Solar flare, in other words called Coronal Mass Ejection(CME), was

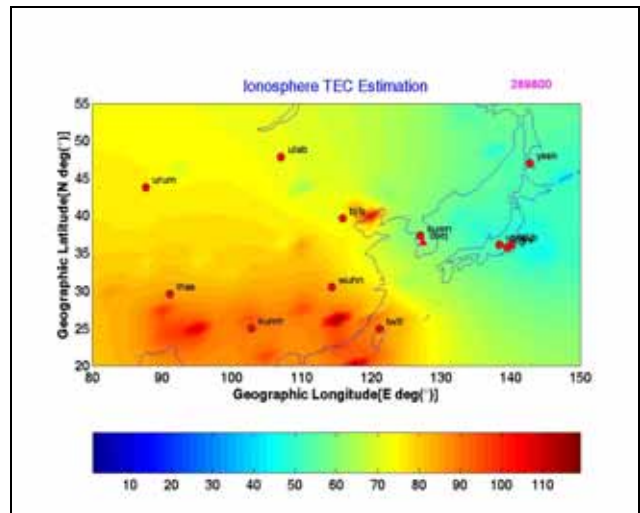


Figure 4. 2D ionosphere Map in north-east Asia at UT 8h

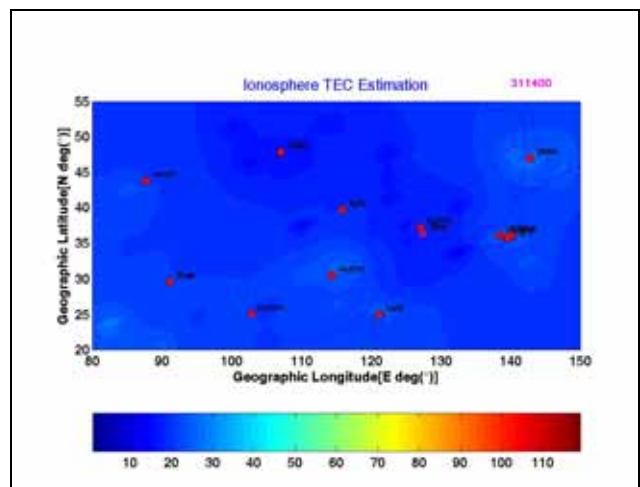


Figure 5. 2D ionosphere Map in north-east Asia at UT 17h

detected and the upper atmosphere of the earth was directly affected by it. Figure 4 and 5 are the results derived from the developed ionospheric model. These images were also provided to show mid-latitude ionospheric activity. Here a geographic reference frame was used to produce the epoch-specific instantaneous regional map of the ionosphere. The obtained ionosphere map has the resolution of 1.25° in latitude and 2.5° in longitude. In contrast to GIMs, this model may observe local features in the ionosphere.

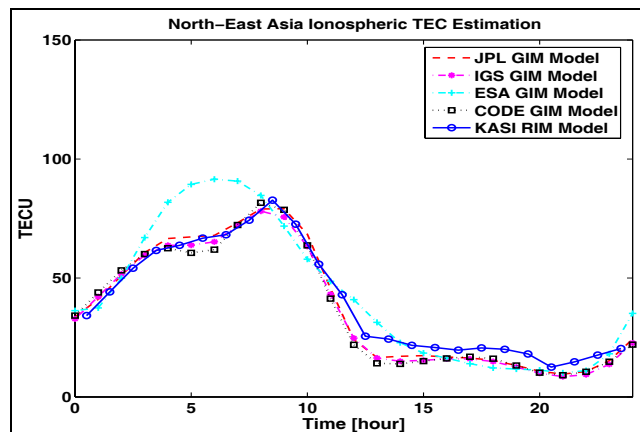


Figure 6. Comparison of VTEC variation at the specific grid point(33.75°N, 112.50°E) on October 29, 2003

As seen in Figure 6, in order to validate the accuracy of the estimated vertical TEC, the comparison to GIMs was performed. As mentioned in the introduction, the time resolution of the GIMs is two-hours generally. So the data of GIMs were conducted the interpolation with one-hour interval. KASI data was also produced in the same way. The compared results are shown in Table 2.

Table 2. Comparison of RMS Values by ionospheric models

Model	RMS(TECU)
KASI-IGS	4.66
KASI-JPL	4.75
KASI-CODE	4.98
KASI-ESA	10.00

The corresponding RMS values are provided in Table 2 and they are all at the TECU(TEC Unit) level. From the obtained results in Table 2, compared to KASI model, IGS, JPL and CODE GIMs showed similar RMS values but there was a large difference with ESA GIMs.

#### 4. Conclusion

North-east Asia ionospheric model has been developed in this research based on grid-based form model. With the sparse IGS sites configuration, the developed model employs a 1.25° 2.5° grid size with the vertical TEC estimation. Compared to GIMs, KASI model has been demonstrated to have some higher spatial resolution and yielded similar RMS values with IGS, JPL and CODE GIMs except ESA GIMs.

Using the IDW method, it is possible to study the regional ionosphere activity and detect the ionospheric phenomenon in the narrow region. However the regional spatial resolution of this model limits the comparison with the data from the global scale.

Lastly, testing under a variety of ionospheric conditions will be preferred in the near future in order to evaluate the performance of the developed model.

#### Acknowledgement

This research was supported by an intrinsic fund of Korea Astronomy and Space Science Institute. I would like also to thank Dr. Joung-Uk Park and Professor Sang-Jeong Lee for their comments on this research.

#### Reference

1. A. Komjathy, *Global Ionospheric Total Electron Content Mapping Using the Global Positioning System*, University of New Brunswick, 1997.
2. A. J. Coster, E. M. Gaposchkin and L. E. Thornton, "Real-Time Ionospheric Monitoring System Using GPS", *Navigation, Journal of Institute of Navigation*, Vo. 39, No. 2, 1992, pp. 191-204.
3. B. D. Wilson, A. J. Mannucci and C. D. Edwards, "Subdaily northern hemisphere ionospheric maps using an extensive network of GPS receivers", *Radio Science*, Vo. 30, 1995, pp. 639-648.
4. G. E. Lanyi and T. Roth, "A comparison of mapped and measured total electron content using global positioning system and beacon satellite observations", *Radio Science*, 1998, Vo. 23, pp. 483-492.
5. J. A. Klobuchar, "Ionospheric Time-Delay Algorithm for

Single-Frequency GPS Users", *IEEE Transactions on Aerospace and Electronics Systems*, Vo. 23, No. 3, 1987, pp. 325-331.

6. J. K. Waler, "Spherical Cap Harmonic Modeling of High Latitude Magnetic Activity and Equivalent Sources with Sparse Observations", *Journal of Atmospheric and Terrestrial Physics*, Vo. 51, No. 2, 1989, pp. 67-80.
7. L. A. Leonovich, K. S. Palamartchouk, N. P. Perevalova and O. M. Pirog, "Observation of large-scale traveling ionospheric disturbances of auroral origin by global GPS networks", *Earth Planets Space*, Vo. 52, 2000, pp. 669-674.
8. M. Fedrizzi, R. B. Langley, A. Komjathy, M.C. Santos, E. R. Paula and I. J. Kantor, "The Low-Latitude Ionosphere: Monitoring its Behavior with GPS", *Proceeding of ION GPS 2001*, Sept. 2004.
9. N. Jakowski, E. Sardon and S. Schluter, "GPS based TEC Observations in Comparison with IRI95 and the European TEC Model NTCM2", *Advances in Space Research*, 1998, Vo 22, pp. 325-331.
10. S. Schaer, *Mapping and Predicting the Earth's Ionosphere Using the Global Positioning System*, University of Berne, 1999.
11. S. Skone, *Wide Area Ionosphere Grid Modeling in the Auroral Region*, Department of Geomatics Engineering, The University of Calgary, 1998.
12. Y. Gao, X. Liao and Z. Liu, "Ionosphere Modeling Using Carrier Smoothed Ionosphere Observations from a Regional GPS Network", *Geomatica*, Vo. 56, 2002, pp. 97-106.
13. X. Liao, *Carrier Phase Based Ionosphere Recovery Over A Regional Area GPS Network*, 2000, The University of Calgary, pp. 248.